Low-Magnitude High-Frequency Vibration Accelerates Callus Formation, Mineralization, and Fracture Healing in Rats

Kwok Sui Leung, Hong Fei Shi, Wing Hoi Cheung, Ling Qin, Wai Kin Ng, Kam Fai Tam, Ning Tang

Department of Orthopaedics and Traumatology, 5/F, Clinical Science Building, Prince of Wales Hospital, The Chinese University of Hong Kong, Shatin, New Territories, Hong Kong SAR, People's Republic of China

Received 28 August 2007; accepted 8 July 2008
Published online in Wiley InterScience (www.interscience.wiley.com). DOI 10.1002/jor.20753

ABSTRACT: Fracture healing is a biological regenerative process that follows a well-orchestrated sequence. Most healing is uneventful and enhancement of normal fracture healing is not commonly done, although it is clinically important in the recovery and regain of functions after fracture. This study investigated the osteogenic effect of low-magnitude high-frequency vibration (LMHFV, 35 Hz, 0.3 *g*) on the enhancement of fracture healing in rats with closed femoral shaft fracture by comparing with sham-treated control. Assessments with plain radiography, micro-CT as well as histomorphometry showed that the amount of callus was significantly larger ($p = 0.001$ for callus area, 2 weeks posttreatment); the remodeling of the callus into mature bone was significantly faster ($p = 0.039$, 4 weeks posttreatment) in the treatment group. The mechanical strength of the healed fracture in the treatment group at 4 weeks was significantly greater ($p < 0.001$). The results showed the acceleration of callus formation, mineralization, and fracture healing in the treatment group. It is concluded that LMHFV enhances healing in the closed femoral shaft fracture in rats. The potential clinical advantages shall be confirmed in the subsequent clinical trials. © Orthopaedic Research Society. Published by Wiley Periodicals, Inc. J Orthop Res

Keywords: low-magnitude high-frequency vibration; fracture healing; callus; femur; remodeling

Fracture healing is a biological regenerative process that follows a well-orchestrated sequence. Most fracture healing is uneventful because it is a very mature biological process with multiple backup mechanisms and alternative pathways. However, complications do occur like delayed unions and nonunions (with an incidence up to 10%).[1,2] Therefore, enhancement of fracture healing has been one of the major goals in modern fracture management because it is clinically important for the recovery and regain of functions after fracture. The biological environment for osteogenic potential, influenced by blood supply,[3] bone-forming cells, growth factors, etc.,[4,5] as well as the mechanical environment[6] are the key determinants for the enhancement of the fracture healing.[7,8] Proper loading conditions have been proven crucial for bone repair and remodeling,[9,10] but the optimal timing and amount of mechanical stimulation remain inconclusive. Low-magnitude high-frequency vibration (LMHFV) is a form of biophysical intervention that provides cyclic loadings. Its osteogenic potential has been proven in animal models[11–16] and clinical trials, with positive effects shown on bone mineral density (BMD),[17–21] blood circulation,[22] muscle functions, and balance control.[23–26] Although the detailed cellular mechanism and molecular pathways remain to be explored,[27,28] this biophysical stimulation does provide noninvasive and systemic effects on musculoskeletal system and its osteogenic effect is promising.[27]

Because fracture healing is a regenerative process of osseous tissue, the osteogenic property of LMHFV may also be effective to enhance this biological process. Therefore, we hypothesized that LMHFV was able to stimulate callus formation and mineralization, and hence to accelerate fracture healing. The aim of this study was to test the osteogenic effects of LMHFV on long bone fracture healing in a closed rat fracture model by comparing with the sham-treated control. The healing status was assessed using plain radiography, with the mineralized callus formation quantified by two-dimensional radiographic analysis and three-dimensional microcomputed tomography (micro-CT). Also, the fracture healing process was evaluated using histomorphometry, with the mechanical outcome assessed by four-point bending tests.

MATERIALS AND METHODS

Rat Facture Model and Experimental Design

Fifty-five 3-month-old female Sprague-Dawley rats, weighting from 200 to 250 g, were used and housed at the Research Animal Laboratory in the authors' institution with 12-h light–night cycle. Free cage movement was allowed with access to standard rat chow and tap water. The Animal Experimentation Ethics Committee of the Chinese University of Hong Kong approved the care and experimental protocol of this study (Ref. No. 06/053/MIS). After 1 week of acclimatization, closed fracture was created following intramedullary pinning in right femoral shaft in each rat according to Einhorn's protocol.[29] Anteroposterior and lateral radiographs were taken to confirm the transverse fracture in the midshaft of the femur postoperatively.

The rats were then randomly assigned to either treatment group or control group. For treatment group, LMHFV therapy was started at day 5 postoperatively, right after the recovery of full weight-bearing standing and walking of the animals. A specially designed vibration platform for animal study was used which provides vertical vibration in 35 Hz with a peak-to-peak magnitude of 0.3 *g* (*g* = gravitational acceleration). The rats were allowed standing separately in bottomless,

Correspondence to: Kwok-Sui Leung (T: 852-2632-2724; F: 852-2637-7889; E-mail: ksleung@cuhk.edu.hk)

compartmented cages fixed on the vibration platform for 20 min/day, 5 days/week. The walls of the cages were opaque and painted in black to minimize the surrounding disturbance. The control group had sham treatment with the rats standing on the vibration platform without switching on the machine using the same regime. At 1, 2, and 4 weeks posttreatment, six rats from each group were euthanized using overdose of sodium pentobarbital and the femora were immediately harvested for the micro-CT and histomorphometric assessments. An additional eight rats from each group were euthanized for mechanical testing at 4 weeks posttreatment.

The transmission of the vibration from paws to thigh in rats was confirmed by using a uniaxial accelerometer (Model 3115A, Dytran Instruments, Chatsworth, CA) attached on the skin surface on the middle of the right thigh in our pilot study. The electrical signals were acquired by the data acquisition system (S/R 500 Hz, Model DI-220, USA). Constant vibration signals (35 Hz) were detected during vibration therapy. Also, the possible effects of sound, magnetic field, and heat produced by the customized vibration platform were assessed. During vibration, the noise produced by the platform was minimal. The intensity of the static magnetic field generated by the platform was measured to be below 1 Gauss on the platform, which was far below the intensity reported to have osteogenic effects[30–34] or the safety level recommended by the Institute of Electrical and Electronics Engineers (IEEE). The thermal effect of the platform was not detected either on the platform surface or within the rat cage after 48 h of continuous running test.

The specific vibration signal (35 Hz, 0.3 *g*) used in this study was chosen according to the previous investigations reported by us[35] and other research groups.[12,36] Briefly, average strain on long bone during daily activity was found to be quite low in magnitude,[37] and these low-level mechanical signals were believed to have profound influence on bone mass and morphology.[38] The 0.3 *g* was regularly used as the magnitude in the other whole-body vibration studies;[12,14,39] therefore, this magnitude was used in the present study. The 30–50 Hz signal, belonging to a relatively high-frequency domain compared with the mechanical signals from muscle contraction, might be critical for maintaining bone mass.[40] Vibration treatment within this frequency domain was found to retard bone loss among postmenopausal women in our previous study,[35] and therefore 35 Hz was chosen as the frequency of interest in this study.

Radiographic Analysis

For the rats euthanized at 4 weeks posttreatment, fracture healing was monitored by weekly anteroposterior and lateral radiography according to established protocol.[41] Two experienced orthopedic surgeons, who were blinded to the animal groupings and time points of the study, performed independent assessments of the fracture healing status of digitized anteroposterior and lateral images from each rat. The radiographic healing was defined as complete mineralized callus bridging of all four cortices on both anteroposterior and lateral radiographs. The external callus width (CW) and callus area (CA) were measured on digitized lateral view images with calibration using Metamorph Image Analysis System (Universal Imaging Corporation, Downingtown, PA).

Micro-CT Analysis

After removal of soft tissues and the intramedullary Kirschner wire, the harvested femora ($n = 6$ for each group at each time point) were scanned by micro-CT system (μCT-40, Scanco Medical, Brüttisellen, Switzerland). The scan range covered 5 mm proximal and 5 mm distal to the fracture line with a resolution of 16 μm per voxel and 1024×1024 pixel image matrices. Contoured region of interest (ROI) was selected in two-dimensional (2D) CT images. Three-dimensional (3D) reconstruction of mineralized tissue was performed using a low-pass Gaussian filter (Sigma = 1.2, Support = 2). To differentiate newly formed mineralized callus from old cortices, the low- and high-density mineralized tissues were reconstructed using different thresholds (high attenuation = 325, low attenuation = 120) defined in 2D images using our recently established evaluation protocol.[42,43] The high-density tissues represented old cortices and newly formed, highly mineralized callus, whereas the low-density tissues represented newly formed callus.[42,43] Quantitative analysis was performed covering the mid 300 slices of the 2D images with the low- and high-density mineralized tissues evaluated separately. Morphometric parameters used for evaluation were total tissue volume (TV, mm^3, calculated from the contoured ROI in 2D images), volume of high-density bone (BV_h, mm^3), volume of low-density bone (BV_l, mm^3), total bone volume (BV_t, mm^3, i.e., equivalent to $BV_h + BV_l$, or TV—interstitial space) and normalized percentage of the tissue volumes including BV_h/TV, BV_l/TV, BV_t/TV.

Histomorphometric Analysis

After micro-CT scanning, the femora were decalcified, cut into halves along the midsagittal plane, and embedded in paraffin. The specimens were then cut in 5 μm-thick sections longitudinally and stained with hematoxylin-eosin (H&E).[41] Each specimen was analyzed with respect to the cellular components in periosteal and fracture areas in two central sections using light microscope system (Leica DMRB DAS, Leica, Heerbrugg, Switzerland).[44] For quantitative analysis, the ROI was evaluated in H&E-stained slides covering 1.5 mm proximal and distal to the fracture line (total 3 mm). The external callus tissues within the ROI were quantified as total callus area (TCA) while the cartilaginous callus area (CCA) was manually defined using Metamorph Image Analysis System (Fig. 4). The percentage of CCA in callus area was expressed as CCA/TCA.

Mechanical Testing

At 4 weeks posttreatment, eight rats from each group were euthanized and the entire femora were dissected free from soft tissues and preserved in gauze with saline and stored at −20°C. In performing the mechanical testing, the femora were thawed overnight at room temperature. The Kirschner wire was removed and the specimen was prepared for four-point bending test. The femora were loaded in the anterior–posterior direction with the posterior side in tension.[45] The inner and outer span of the blades was 8 and 20 mm, respectively, with the long axis of the femora oriented perpendicular to the blades during the test. A constant displacement rate of 5 mm/min was used to test the femora to failure using a material test machine (H25KS Hounsfield Test Equipment Ltd. Redhill, Surrey, UK). The ultimate load (UL) and stiffness were recorded and analyzed using built-in software (QMAT Professional Material testing software. Hounsfield Test Equipment Ltd. Redhill, Surrey, UK).

Statistical Analysis

All quantitative data were expressed as mean ± standard error (SE) and analyzed with SPSS version 13.0 software (SPSS Inc, Chicago. IL). Independent t-test was used to compare the differences between treatment and control groups at corresponding time points. Significant difference was set at a probability level of 95% ($p < 0.05$).

RESULTS

All rats resumed partial weight bearing within a few hours after surgery. All rats recovered full weight-bearing walking before the start of vibration or sham treatment (day 5 postoperatively). During treatments, the rats stood calmly with both hind paws on the vibration platform without panic behaviors. No significant difference in body weight was observed between groups in the study period. Of the 55 operated rats, one died and two were excluded due to nontransverse fractures created; thus, 52 rats were included in the study.

Radiographic Analysis

Obvious radio-opaque external callus around the fracture site was observed in both groups from 1 week posttreatment and throughout the study period. Compared with the control, the vibration treatment group showed a faster bridging of callus gaps in the serial lateral radiographies (Fig. 1). For the healing status, at 3 weeks posttreatment, 50% (7/14) of the rats in the treatment group and 21.4% (3/14) in the control showed radiographic healing. At 4 weeks posttreatment, 85.7% (12/14) in the treatment group and 57.1% (8/14) in the control showed radiographic healing. For quantitative analysis, at 1 week posttreatment, the treatment group presented 22.5% larger CW ($p = 0.003$) and 29.7% larger CA ($p = 0.004$) compared with the control (Fig. 2). At 2 weeks posttreatment, CW and CA increased in both groups with the treatment group showing 21.1% larger CW and 25.1% larger CA than the control ($p < 0.001$ and $p = 0.001$, respectively). At 3 weeks posttreatment, CW and CA decreased in both groups. Difference in CW between groups was no longer significant, while larger CA ($p = 0.004$) still presented in the treatment group (Fig. 2). By 4 weeks posttreatment, the treatment group showed smaller CW, larger CA, and flatter shape of the external calluses compared with the control. No significant difference was found between groups at this time point (Fig. 2).

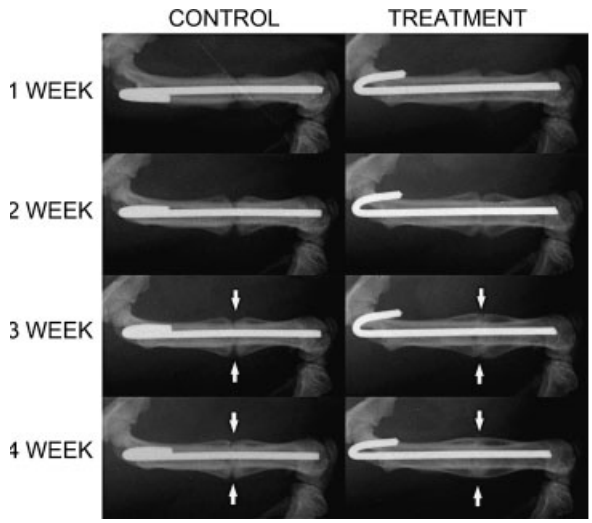

Figure 1. Series of representative lateral radiographs at different time points showing a faster healing process in the treatment group than in the control. At 3 weeks posttreatment, the callus gaps (white arrows) in the treatment group presented a smaller size than those in the control. At 4 weeks posttreatment, the fracture was completely bridged by mineralization callus in the treatment group with the disappearance of callus gaps. While in the control group, callus gaps remained at the fracture site (white arrows).

Mcro-CT Aalysis

At different time points, reconstructed mineralized calluses showed different morphologic characteristics between groups in the 3D micro-CT images (Fig. 3). At 1 week posttreatment, newly formed callus (low-density bone) appeared in the perifracture region, together with a larger callus gap in the treatment group compared with the control (Fig. 3). The quantitative measurements of TV and BV_1 showed higher values in the

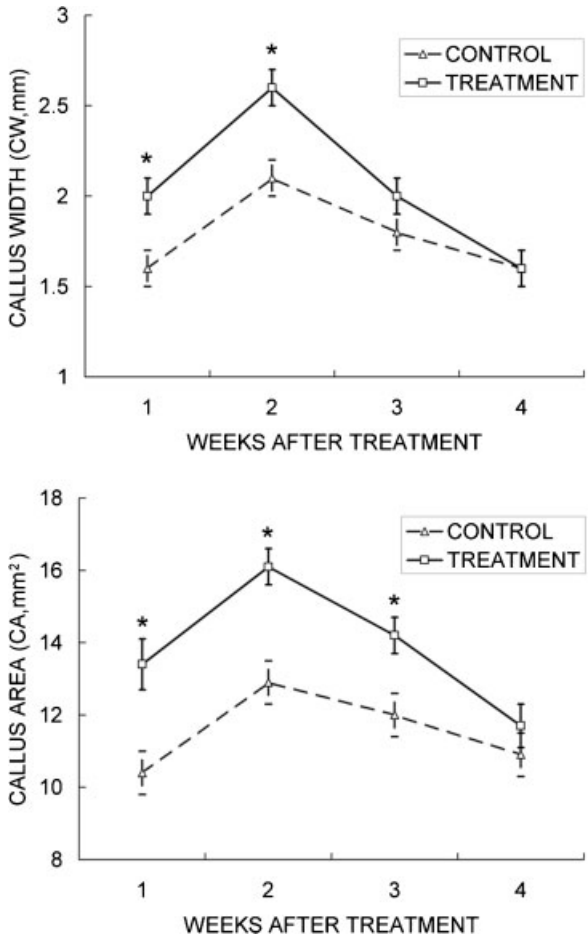

Figure 2. Temporal changes of callus width (CW) and callus area (CA) measured in laterial radiographs in the treatment group and the control. (*$p < 0.05$, independent samples t-test; error bar: ± SE).

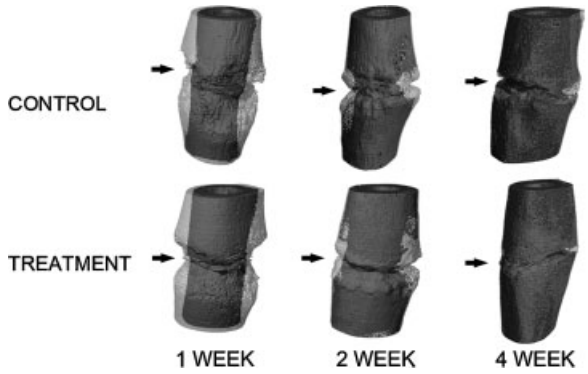

Figure 3. Series of representative micro-CT images showing 3D architectures of fracture fragment and external callus at different time points. In each image, the high-density bone (threshold >325, representing the old cortices and highly mineralized callus) was shown in dark color, while the low-density bone (threshold 120–325, representing the newly formed callus) was shown in trensparent light color. The unmineralized tissue (threshold <120) was not shown. At 1 week posttreatment, newly formed callus (low-density bone) was observed in both groups, while the vibration group showed a larger callus gap at fracture site than the control (black arrows). At 2 weeks posttreatment, remarkable callus formation was observed in both groups, while the treatment group showed a more regular, symmetrical, and complete appearance with a smaller callus gap completely bridged by mineralized callus (low-density bone) in the treatment group, compared with the callus gaps left in the control (balck arrows).

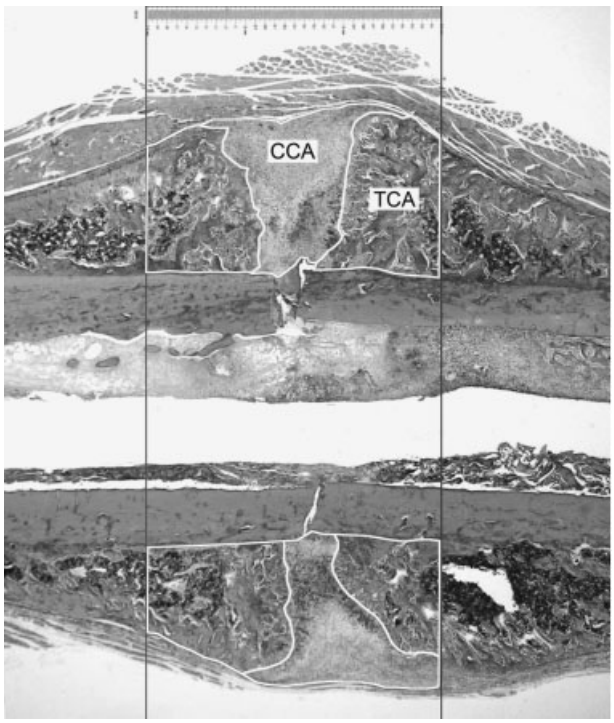

Figure 4. Histomorphometric analysis in midsagittal section of the healing femoral shaft fracture stained with H&E (16×). The outer rectangle marked the ROI covering 1.5 mm proximal and distal to the fracture line (total 3 mm), for callus area quantification. The cartilaginous callus area (CCA) and total callus area (TCA) were measured manually within the ROI using the Metamorph Image Analysis System.

treatment group, but the differences were not statistically significant (Table 1). At 2 weeks posttreatment, remarkable callus formation was observed in both groups while the treatment group showed more regular, symmetrical, and complete appearance with a smaller callus gap at fracture site (Fig. 3). Quantitatively, 15.3% larger BV_t and 21.4% larger BV_l were observed in the treatment group at this time point ($p = 0.025$ and 0.004, respectively), while TV demonstrated slightly higher value yet not statistically significant (Table 1). At 4 weeks posttreatment, the callus gaps were completely bridged by mineralized callus (low-density bone) in the treatment group, compared with the persistent callus gaps left in the control (Fig. 3). The treatment group presented 32.8% larger BV_h and 24.8% higher BV_h/TV than the control with $p = 0.026$ and 0.017, respectively (Table 1).

Histomorphometric Analysis

All samples demonstrated secondary fracture healing with callus formation and endochondral ossification. In both groups, newly formed woven bone, blood vessels, and enlarged osteoblasts were observed beneath the periosteum adjacent to the fracture site at 1 week posttreatment. Cartilaginous tissue filled the fracture site, presented as the callus gap observed in radiography and micro-CT, with proliferating chondrocytes around the periosteal woven bone. Quantitatively, significantly larger TCA, CCA, and CCA/TCA were observed in treatment group ($p = 0.011$, $p < 0.001$, and $p < 0.001$ respectively) (Table 1). At 2 weeks posttreatment, more periosteal woven bone was observed around the fracture site in both groups, with early remodeling of the trabecular bone appeared adjacent to the woven bone. The width of the cartilaginous tissue decreased and active endochondral ossification was present between the cartilaginous tissue and the woven bone. Significantly larger TCA was observed in the treatment group ($p = 0.039$), whereas CCA and CCA/TCA showed no significant difference between groups (Table 1). In the control group of week 4 posttreatment samples, cartilage filled the fracture site while endochondral ossification was still present in the unhealed fracture. In the treatment group, woven bone replaced the cartilaginous tissue with complete bridging by osseous tissue at the fracture site in the most of the samples. No significant difference was found between groups in TCA, CCA, or CCA/TCA at this time point (Table 1).

Mechanical Testing

Typical load–displacement curve of long bone was confirmed in all the individual bending tests performed on the fractured femora showing an initial short nonlinear response (preloading or engaging) followed by an upward-sloping linear component (elastic phase) and then a failure response at the break point. The UL of the treatment group was 50.1% higher compared with the

Table 1. Fracture Callus Quantified by Micro-CT and Histomorphometry (data in mean ± SE, $n = 6$)

		Week 1		Week 2		Week 4	
Parameter		Control	Vibration	Control	Vibration	Control	Vibration
Micro-CT[b]	TV (mm^3)	87.4 ± 4.3	97.9 ± 4.6	109.0 ± 3.3	121.4 ± 4.8	102.3 ± 5.6	105.9 ± 6.4
	BV_t (mm^3)	58.7 ± 3.2	63.7 ± 2.6	75.1 ± 2.1	86.6 ± 3.3[a]	76.6 ± 3.0	87.3 ± 8.0
	BV_l (mm^3)	36.7 ± 3.0	41.4 ± 2.9	49.6 ± 1.0	60.2 ± 2.3[a]	43.3 ± 3.4	44.9 ± 3.4
	BV_h (mm^3)	22.0 ± 0.4	22.4 ± 0.5	25.5 ± 2.0	26.4 ± 1.6	33.2 ± 0.9	44.1 ± 3.9[a]
	BV_t/TV (%)	67.2 ± 2.0	65.3 ± 1.5	68.9 ± 0.7	71.5 ± 1.7	75.2 ± 1.5	81.7 ± 2.8
	BV_l/TV (%)	41.8 ± 2.0	42.0 ± 1.4	45.7 ± 1.5	49.8 ± 1.6	42.1 ± 1.1	42.3 ± 1.1
	BV_h/TV (%)	25.4 ± 1.2	23.2 ± 1.6	23.3 ± 1.3	21.7 ± 0.9	33.1 ± 2.4	41.3 ± 1.6[a]
Histomorphometry	TCA (mm^2)	6.9 ± 0.2	8.0 ± 0.2[a]	8.4 ± 0.2	9.6 ± 0.4[a]	6.4 ± 0.4	6.1 ± 0.2
	CCA (mm^2)	3.8 ± 0.1	6.0 ± 0.2[a]	2.7 ± 0.2	3.0 ± 0.2	0.3 ± 0.1	0.0 ± 0.0
	CCA/TCA (%)	54.2 ± 1.7	75.1 ± 1.8[a]	32.7 ± 1.8	31.5 ± 1.4	4.5 ± 2.2	0.0 ± 0.0

[a] $p < 0.05$ (independent samples t-test); [b] In micro-CT quantification, the volume of cartilaginous tissue in callus is not included.

control group ($p = 0.023$) and 67.3% higher stiffness was observed in the treatment group ($p = 0.001$) (Table 2).

DISCUSSION

LMHFV is a form of biophysical stimulation delivering noninvasive, systemic, and cyclic mechanical stimuli.[46] Its osteogenic effect on intact bone and stimulative effect on limb blood flow have been documented in animal and human studies,[12,21,22] which are considered to be essential in fracture healing. The present study investigated the effects of LMHFV on fracture healing in a closed rat femoral shaft fracture model with the findings indicating a significant enhancement in fracture healing. The healing process in the treatment group was accelerated with enhanced callus formation and faster callus mineralization when compared with the control. This is the first evidence showing fracture healing enhancement with the application of LMHFV.

Mechanical stimulation is known to have osteogenic effects. Although a variety of methods and clinical facilities in mechanical or biophysical forms have been developed to enhance fracture healing,[46,47] gap remains in the search of a practical enhancement possessing that could be noninvasive and effective with well-defined specifications and regimes. Comparing with other forms of enhancements, the application of LMHFV may have special indication in enhancement of fracture healing because of its noninvasiveness with systemic and osteogenic charecteristics.[48]

Table 2. Results of Four-Point Bending of the Femora at the End of 4 Weeks Treatment (Data in Mean ± SE, $n = 8$)

	Week 4	
Parameter	Control	Vibration
Ultimate load (N)	96.4 ± 12.9	144.7 ± 13.9[a]
Stiffness (N/mm)	177.8 ± 22.9	288.5 ± 9.8[a]

[a] $p < 0.05$ (Independent samples t-test).

In this study, the animals were treated with the standard regime of LMHFV and showed positive effects on fracture healing. The animals were subjected to vibration stimulation, which was confirmed by the detection of the signal transmission at the midthigh level by an accelerometer. The enhancement of fracture healing in animals treated with LMHFV is shown by the increased callus formation after 1 eek of treatment in which both the callus width and the area were significantly increased as compared with the control. The callus width decreased much faster in the later phase of the treatment. This is explained by the faster mineralization and remodeling of the callus in the treatment group. The radiographic data were further confirmed by the micro-CT analysis where the enhancement of fracture healing in the treatment group was demonstrated at 1 week posttreatment despite the difference not reaching statistically significant level. At 2 weeks posttreatment, while the volumes of the high-density bone (the original bone ends) (BV_h) were similar in both groups, the low-density bone (BV_l) and the total bone volume (BV_t) around the fracture site increased significantly in the treatment group, indicating that the callus formation was much stimulated following LMHFV treatment. At 4 weeks posttreatment, while the normal fracture healing was progressing into callus remodeling, the treatment group showed significant increase in the volume of high-density bone (BV_h) and the ratio of volume of high-density bone to the total tissue volume (BV_h/TV). The total tissue volume (TV) and total bone volume (BV_t) in both groups also increased with the treatment group remaining higher, although the differences were not statistically significant. This indicated that the callus formed in the treatment group mineralized and matured faster than the control at the later phase (133.6% faster at 3 weeks and 50.1% more complete callus bridging at 4 weeks posttreatment).

Histomorphometrically, the area of cartilaginous callus (CCA) was larger in the treatment group at 1 week posttreatment. The TCA and the CCA were found significantly larger in the treatment group, indicating a positive stimulation on callus formation from the very beginning of the fracture healing. At 2 weeks posttreatment, while the TCA was significantly larger; the CCA, however, did not show difference from the control group. This echoed with the increased BV_l and BV_t in micro-CT analysis. At week 4, cartilaginous callus was almost not found in the treatment group, which explained the significantly higher BV_h detected in micro-CT analysis, indicating that the massive callus mineralization induced by the LMHFV was much faster than the control.

The biomechanical property of the healed fracture was tested with a four-point bending test. The results again confirmed that the fracture healed under LMHFV was mechanically 50.1% ($p < 0.05$) stronger than the control at 4 weeks posttreatment, indicating the acceleration of fracture healing in the treatment group that resulted in a stronger structure.

This study confirmed the positive effect of LMHFV on fracture healing in the closed femoral shaft fracture in rats. Although we did not investigate the molecular biology and the mechanism of the stimulation in the present study, the mechanical stimulation provided by the LMHFV may be involved in stimulation of blood flow in the muscles which surrounded the fracture site, thus providing a better biological environment for fracture healing.[22] The mechanical stimuli to the fracture ends may also induce more endochondral ossification as depicted by a larger cartilaginous callus in early phase of the healing. The increased rate of callus mineralization may reflect the positive effect on cell differentiation as shown in our previous study with low-intensity pulsed ultrasound (LIPUS) on periosteal cells.[49] Further studies on gene expression are undergoing in our institute to understand the different responses of the osseous tissues to LMHFV during fracture healing.

The rate of fracture healing induced by LMHFV was improved by 25–30%, which could have tremendous potential for clinical application. This effect is comparable to that from LIPUS stimulation,[50] which has the limitation of local application on fractures with thin soft tissues envelope like tibia or distal radius. The application of LMHFV may have wider application because its effect is more systemic. Faster healing will facilitate earlier rehabilitation and regain of functions after fracture. The stimulatory effects may decrease the incidence of delayed union or nonunion, which is common in fractures resulted from high energy trauma like open fractures. A faster fracture healing rate will also lead to a decrease in the implant failure rate. All these will help to minimize the cost of treating fractures, which are still the commonest cause of loss of working force in the society where younger generation is prime victims.

Beneficial effect of vibration was also reported in Goodship's study in which axial interfragmentary movement of 0.02 mm at 32 Hz (30,000 loading cycles) was confirmed to enhance endochondral bone repair with an ovine tibial open osteotomy model.[48] However, Wolf et al.[51] only found slight but insignificant difference of metatarsal osteotomy healing under 0.02 mm of interfragmentary movements at 20 Hz (6000 loading cycles). Disagreement in the results of these studies, as explained by Wolf et al.,[51] were probably due to the different setups of treatment specifications and regimes. In the current study, positive effects of LMHFV were testified in a closed fracture model, which was different from the open osteotomy models[48,51] because the fracture hematoma was undisturbed and the soft tissue damage was minimal in the closed fracture model.[29,52]

This study has a few limitations. First, we managed to detect the transmission of vibration signal at midthigh level of the rats, but neither real-time nor spot check of interfragmentary strain at fracture site on conscious rats in movements was done due to limited technology. Second, only the effects of LMHFV on diaphyseal fractures were addressed in this study. The stimulatory effect of LMHFV might not be able to apply directly to metaphyseal fractures. Third, investigation on the effect of LMHFV during the initiation of fracture healing was not addressed in this study because LMHFV treatment was not started immediately after surgery due to the fact that it took around 5 days for the rats to recover full weight-bearing standing and walking on the fractured limb. This time point also echoed the stabilization of hematoma and early angiogenesis.[53,54]

In conclusion, the healing of the closed femoral shaft fractures in the rat model was significantly enhanced with low-magnitude high-frequency vibration. The enhancement was illustrated with positive osteogenic effect by formation of larger amount of callus, accelerated callus remodeling, and finally a complete restoration of stronger osseous tissue around the fracture site. These findings would imply that the anabolic effect of vibration treatment on fracture healing might have great potential in clinical applications.

ACKNOWLEDGMENTS

This study was supported by Hong Kong Research Grant Council Earmarked Grant (CUHK 4502/06M) and AIOD Research Grant (050805 KSWH). The authors would like to thank the Technical Services Units of the Chinese University of Hong Kong in constructing the vibration platforms for this study; Prof. Benson Yeung and Mr. Simon Chow for their help in micro-CT scanning; and Miss Winnie Lee for her help in histomorphometric analysis.

REFERENCES

1. Leung KS, Ko PS. 2001. Practical manual for musculoskeletal trauma. Berlin: Springer.
2. Westerhuis RJ, van Bezooijen RL, Kloen P. 2005. Use of bone morphogenetic proteins in traumatology. Injury 36(12):1405–1412.
3. Glowacki J. 1998. Angiogenesis in fracture repair. Clin Orthop Relat Res 355(Suppl):S82–S89.

4. Caplan AI. 1991. Mesenchymal stem cells. J Orthop Res 9: 641–650.
5. Hulth A. 1989. Current concepts of fracture healing. Clin Orthop Relat Res 249:265–284.
6. Claes LE, Heigele CA, Neidlinger-Wilke C, et al. 1998. Effects of mechanical factors on the fracture healing process. Clin Orthop Relat Res 355(Suppl):S132–S147.
7. Hannouche D, Petite H, Sedel L. 2001. Current trends in the enhancement of fracture healing. J Bone Joint Surg Br 83: 157–164.
8. Marsh DR, Li G. 1999. The biology of fracture healing: optimising outcome. Br Med Bull 55:856–869.
9. Cowin SC. 1986. Wolff's law of trabecular architecture at remodeling equilibrium. J Biomech Eng 108:83–88.
10. Chao EY, Inoue N, Elias JJ, et al. 1998. Enhancement of fracture healing by mechanical and surgical intervention. Clin Orthop Relat Res 355(Suppl):S163–S178.
11. Oxlund BS, Ortoft G, Andreassen TT, et al. 2003. Low-intensity, high-frequency vibration appears to prevent the decrease in strength of the femur and tibia associated with ovariectomy of adult rats. Bone 32:69–77.
12. Rubin C, Turner AS, Bain S, et al. 2001. Anabolism. Low mechanical signals strengthen long bones. Nature 412:603–604.
13. Flieger J, Karachalios T, Khaldi L, et al. 1998. Mechanical stimulation in the form of vibration prevents postmenopausal bone loss in ovariectomized rats. Calcif Tissue Int 63:510–514.
14. Christiansen BA, Silva MJ. 2006. The effect of varying magnitudes of whole-body vibration on several skeletal sites in mice. Ann Biomed Eng 34:1149–1156.
15. Rubin C, Turner AS, Muller R, et al. 2002. Quantity and quality of trabecular bone in the femur are enhanced by a strongly anabolic, noninvasive mechanical intervention. J Bone Miner Res 17:349–357.
16. Judex S, Lei X, Han D, et al. 2007. Low-magnitude mechanical signals that stimulate bone formation in the ovariectomized rat are dependent on the applied frequency but not on the strain magnitude. J Biomech 40:1333–1339.
17. Ward K, Alsop C, Caulton J, et al. 2004. Low magnitude mechanical loading is osteogenic in children with disabling conditions. J Bone Miner Res 19:360–369.
18. Iwamoto J, Takeda T, Sato Y, et al. 2005. Effect of whole-body vibration exercise on lumbar bone mineral density, bone turnover, and chronic back pain in post-menopausal osteoporotic women treated with alendronate. Aging Clin Exp Res 17:157–163.
19. van Nes IJ, Latour H, Schils F, et al. 2006. Long-term effects of 6-week whole-body vibration on balance recovery and activities of daily living in the postacute phase of stroke: a randomized, controlled trial. Stroke 37:2331–2335.
20. Gilsanz V, Wren TA, Sanchez M, et al. 2006. Low-level, high-frequency mechanical signals enhance musculoskeletal development of young women with low BMD. J Bone Miner Res 21: 1464–1474.
21. Rubin C, Recker R, Cullen D, et al. 2004. Prevention of postmenopausal bone loss by a low-magnitude, high-frequency mechanical stimuli: a clinical trial assessing compliance, efficacy, and safety. J Bone Miner Res 19:343–351.
22. Stewart JM, Karman C, Montgomery LD, et al. 2005. Plantar vibration improves leg fluid flow in perimenopausal women. Am J Physiol Regul Integr Comp Physiol 288:R623–R629.
23. Verschueren SM, Roelants M, Delecluse C, et al. 2004. Effect of 6-month whole body vibration training on hip density, muscle strength, and postural control in postmenopausal women: a randomized controlled pilot study. J Bone Miner Res 19:352–359.
24. Torvinen S, Kannus P, Sievanen H, et al. 2003. Effect of 8-month vertical whole body vibration on bone, muscle performance, and body balance: a randomized controlled study. J Bone Miner Res 18:876–884.
25. Blottner D, Salanova M, Puttmann B, et al. 2006. Human skeletal muscle structure and function preserved by vibration muscle exercise following 55 days of bed rest. Eur J Appl Physiol 97:261–271.
26. Cheung WH, Mok HW, Qin L, et al. 2007. High-frequency whole-body vibration improves balancing ability in elderly women. Arch Phys Med Rehabil 88:852–857.
27. Rubin C, Judex S, Qin YX. 2006. Low-level mechanical signals and their potential as a non-pharmacological intervention for osteoporosis. Age Ageing 35(Suppl 2):ii32–ii36.
28. Judex S, Zhong N, Squire ME, et al. 2005. Mechanical modulation of molecular signals which regulate anabolic and catabolic activity in bone tissue. J Cell Biochem 94:982–994.
29. Bonnarens F, Einhorn TA. 1984. Production of a standard closed fracture in laboratory animal bone. J Orthop Res 2:97–101.
30. Bruce GK, Howlett CR, Huckstep RL. 1987. Effect of a static magnetic field on fracture healing in a rabbit radius. Preliminary results. Clin Orthop Relat Res 222:300–306.
31. Yan QC, Tomita N, Ikada Y. 1998. Effects of static magnetic field on bone formation of rat femurs. Med Eng Phys 20:397–402.
32. Kotani H, Kawaguchi H, Shimoaka T, et al. 2002. Strong static magnetic field stimulates bone formation to a definite orientation in vitro and in vivo. J Bone Miner Res 17:1814–1821.
33. Puricelli E, Ulbrich LM, Ponzoni D, et al. 2006. Histological analysis of the effects of a static magnetic field on bone healing process in rat femurs. Head Face Med 2:43.
34. Costantino C, Pogliacomi F, Passera F, et al. 2007. Treatment of wrist and hand fractures with natural magnets: preliminary report. Acta Biomed 78:198–203.
35. Sze PC, Mok HW, Cheung WH, et al. 2008. Effectiveness of low-magnitude high-frequency vibration in retardation of bone loss and improvement of balancing ability among postmenopausal women. 54th Annual Meeting of the Orthopaedic Research Society: Paper No. 275.
36. Judex S, Donahue LR, Rubin C. 2002. Genetic predisposition to low bone mass is paralleled by an enhanced sensitivity to signals anabolic to the skeleton. FASEB J 16:1280–1282.
37. Fritton SP, McLeod KJ, Rubin CT. 2000. Quantifying the strain history of bone: spatial uniformity and self-similarity of low-magnitude strains. J Biomech 33:317–325.
38. Qin YX, Rubin CT, McLeod KJ. 1998. Nonlinear dependence of loading intensity and cycle number in the maintenance of bone mass and morphology. J Orthop Res 16:482–489.
39. Judex S, Boyd S, Qin YX, et al. 2003. Adaptations of trabecular bone to low magnitude vibrations result in more uniform stress and strain under load. Ann Biomed Eng 31:12–20.
40. Huang RP, Rubin CT, McLeod KJ. 1999. Changes in postural muscle dynamics as a function of age. J Gerontol A Biol Sci Med Sci 54:B352–B357.
41. Leung KS, Cheung WH, Yeung HY, et al. 2004. Effect of weightbearing on bone formation during distraction osteogenesis. Clin Orthop Relat Res 419:251–257.
42. Yingjie H, Ge Z, Yisheng W, et al. 2007. Changes of microstructure and mineralized tissue in the middle and late phase of osteoporotic fracture healing in rats. Bone 41:631–638.
43. Gabet Y, Muller R, Regev E, et al. 2004. Osteogenic growth peptide modulates fracture callus structural and mechanical properties. Bone 35:65–73.

44. Chan CW, Qin L, Lee KM, et al. 2006. Dose-dependent effect of low-intensity pulsed ultrasound on callus formation during rapid distraction osteogenesis. J Orthop Res 24:2072–2079.
45. Volkman SK, Galecki AT, Burke DT, et al. 2004. Quantitative trait loci that modulate femoral mechanical properties in a genetically heterogeneous mouse population. J Bone Miner Res 19:1497–1505.
46. Chao EY, Inoue N. 2003. Biophysical stimulation of bone fracture repair, regeneration and remodelling. Eur Cells Mater 6:72–84; discussion 84–75.
47. Khan Y, Laurencin CT. 2008. Fracture repair with ultrasound: clinical and cell-based evaluation. J Bone Joint Surg 90 (Suppl 1):138–144.
48. Goodship A, Rubin C. 1997. Low magnitude high frequency mechanical stimulation of endochondral bone repair. Trans Orthop Res Soc 43:234.
49. Leung KS, Cheung WH, Zhang C, et al. 2004. Low intensity pulsed ultrasound stimulates osteogenic activity of human periosteal cells. Clin Orthop Relat Res 418:253–259.
50. Leung KS, Lee WS, Tsui HF, et al. 2004. Complex tibial fracture outcomes following treatment with low-intensity pulsed ultrasound. Ultrasound Med Biol 30:389–395.
51. Wolf S, Augat P, Eckert-Hubner K, et al. 2001. Effects of high-frequency, low-magnitude mechanical stimulus on bone healing. Clin Orthop Relat Res 385:192–198.
52. Park SH, O'Connor K, Sung R, et al. 1999. Comparison of healing process in open osteotomy model and closed fracture model. J Orthop trauma 13:114–120.
53. Gardner MJ, Ricciardi BF, Wright TM, et al. 2008. Pause insertions during cyclic in vivo loading affect bone healing. Clin Orthop Relat Res 466:1232–1238.
54. Wallace AL, Draper ER, Strachan RK, et al. 1994. The vascular response to fracture micromovement. Clin Orthop Relat Res 301:281–290.